Recent advances in Fragment-based strategies against tuberculosis

Baptiste Villemagne, Léo Faïon, Salia Tangara, Nicolas Willand

Recent advances in Fragment-based strategies against tuberculosis

Baptiste Villemagne[1], Léo Faion[1], Salia Tangara[1], Nicolas Willand[1]

[1] Univ. Lille, Inserm, Institut Pasteur de Lille, U1177 - Drugs and Molecules for Living Systems, F-59000, Lille, France.

Corresponding author: Villemagne,B. (baptiste.villemagne@univ-lille.fr)

Keywords : Tuberculosis, Fragments, Fragment-based drug design, review

Abstract

Tuberculosis remains one of the world's leading infectious disease killers, causing more than 1.5 million of deaths each year. It is therefore a priority to discover and develop new classes of anti-tuberculosis drugs to design new treatments in order to fight the increasing burden of resistant-tuberculosis. Fragment-based drug discovery (FBDD) relies on the identification of small molecule hits, further improved to high-affinity ligands through three main approaches: fragment growing, merging and linking. The aim of this review is to highlight the recent progresses made in fragment-based approaches for the discovery and development of *Mycobacterium tuberculosis* inhibitors.

Introduction

Tuberculosis (TB), caused by the pathogen *Mycobacterium tuberculosis* (*M.tb*), has been part of mankind history for centuries. The 20th century represented a watershed in the evolution of the disease with the improvement of hygiene and standard of living in parallel of the discovery of the BCG vaccine and the first antibiotics, leading to a decline in the spread of the disease. Unfortunately, with the rise of drug-resistance and the epidemic of HIV, the 1980's witnessed a resurgence of TB. In order to reverse the trend, the WHO declared TB as a global health emergency at the end of the 20th century, and launched the stop TB program, which has been continued by the End TB program in 2015. This program aims to reduce by 90% the number of TB deaths between 2015 and 2030. Thanks to the increasing efforts from the WHO in the past two decades, the number of deaths has been reduced by 14% between 2015 and 2020[1], far from the initial 35% reduction 2020 milestone. However, the coronavirus disease (COVID-19) pandemic has threatened these gains by causing important disruption to services (treatment and diagnosis), reversing gains and setting back the fight against TB by several years. As a consequence, TB remains one of the top 10 causes of death worldwide, with 10.0 million people infected in 2020, and 1.5 million (including 0.214 million co-infected with HIV) died from TB the same year.[2]

One major challenge for treating tuberculosis is the long duration of the treatment with the current front-line combination of drugs (6 months), which does not facilitate compliance, and thus precludes the selection of multi-drug resistant (MDR) and extensively drug resistant (XDR) strains. The massive escalating emergence of these resistant strains of *M.tb,* over the last decades, resulted in 483,000 cases of rifampicin-resistant TB reported in 2020[2] as well as 12,350 cases of extensively drug resistant (XDR) TB reported in 2019[1]. When multidrug resistance is diagnosed, patients have to undergo a 2-year regimen with cure rates of only 50% for MDR-TB and 20% for XDR-TB.

It is therefore crucial to find new drugs acting through new mechanisms of action. Ideally, these drugs would: 1) be active against MDR and XDR strains, 2) be able to improve and shorten the first-line treatments, 3) target non-replicating bacilli and 4) be compatible with

other drugs to be used in antitubercular and anti-HIV combination treatments. Concerted drug discovery efforts since the 2000's allowed the clinical development and approval of two novel classes of anti-TB drugs, namely, bedaquiline (BDQ)[3], and nitroimidazoles (delamanid and pretomanid)[4]. In addition to these, a number of promising compounds have been added to the pre-clinical and clinical anti-TB drug discovery pipeline in the last 15 years[5]. In order to accelerate the development of new regimens for the treatment of tuberculosis, a European public-private platform (ERA4TB) has been launched. However, this pipeline remains sparsely filled, and will need additional lead compounds with new modes of action to develop novel combination therapies.

Fragments-based drug design (FBDD), relying on the screening of small libraries (usually 1 000 to 10 000 compounds) of low molecular weight molecules (heavy atom count (HAC) < 17-20) is now a well-established process in both industry and academia.[6] It is often used in drug discovery programs together with standard HTS approaches, where large libraries (10^5-10^7 compounds) of lead-like and drug-like molecules (HAC 25-35) are screened, or with other hit finding approaches. There are several advantages in the use of small molecules as drug discovery programs starting points. First of all, the sampling of chemical space is much more efficient with fragments, even with a small number of them (10^3-10^4).[7] Moreover, the assembling and use of such small libraries is of course less costly and therefore accessible to most academics and small biotech companies, on top of the pharmaceutical industry. In addition, these small chemical entities usually display more efficient binding modes[8] and tend to display better physicochemical properties (such as solubility), which is known to be a major reason of compounds failure in clinical trials.[9] As a consequence of the numerous advantages mentioned hereabove, fragment-based programs often lead to quicker lead optimization. This optimisation can be achieved through three main strategies: fragment-growing, fragment-linking and fragment-merging. Fragment-growing is predominantly used as it simply involves the "growing" of an initial hit fragment, by expending the structure in order to find new interactions within the ligand binding domain. This process is highly facilitated when binding mode information is available, allowing for an easier target of surrounding binding pockets. When several fragments occupy non-overlapping binding sites, they can be assembled in a fragment-linking strategy. Finally, fragment merging consists in merging structural features of fragments overlapping with other known ligands. The recent advances regarding the three key aspects of fragment-based approaches: Fragment-library design, detection of fragment hits and fragment-to-lead strategies is very well documented.[10]

To date, FBDD has produced 4 approved drugs[11] and tens of drug candidates which originate from fragments are currently undergoing clinical trials. Although FBDD has been mainly applied to proteins involved in cancer (especially kinases), it is also a very attractive approach for the discovery of new antibiotics.[12] *M.tb* has a very particular hydrophobic and poorly permeable envelope due to a unique mycolic acid layer.[13] Therefore cell penetration has become a major challenge in the identification of new antitubercular drugs, and is often

responsible for the frustrating lack of transposition from the “on-target” activity of hits or lead compounds to their whole cell activity. To this extend, fragments represent an attractive source of small and moderately lipophilic molecules which are more likely to penetrate into the bacteria through porins.[14]

The first examples of fragment-based approaches for the discovery of new *M.tb* inhibitors were described in the late 2000s, with the discovery of inhibitors of tyrosine phosphatases MPtpA and MPtpB.[15] Since then, FBDD has been applied to many other targets and pathways for the discovery of new antitubercular agents Figure 1).[16] In this review, we will discuss the most recent advances in fragment-based approaches applied to the discovery and development of *M.tb* inhibitors.

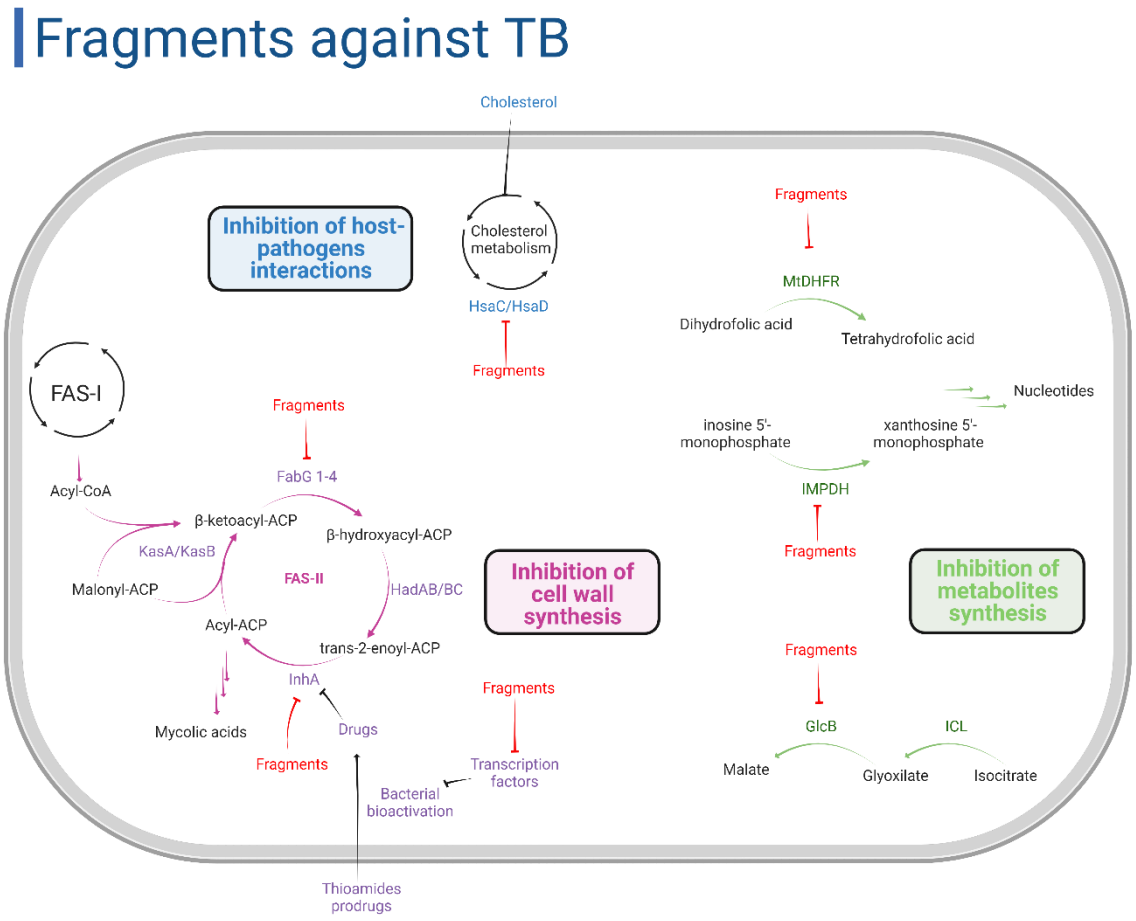

Figure 1 : Recent fragment-based approaches against *Mycobacterium tuberculosis*.

Development of Fragments targeting cell wall-synthesis

The best example to illustrate the interest of working with fragments is that a large part of anti-tuberculosis drugs, targeting the cell-wall synthesis, are rule of three compliant molecules such as ethambutol, isoniazid, ethionamide or prothionamide. The first one is a first line drug that inhibits arabinogalactan biosynthesis (through inhibition of arabinosyl transferase). The three others are prodrugs, meaning that they are bioactivated within the bacteria into their active form. This is the case of the first line prodrug isoniazid (INH) and second line prodrugs ethionamide (ETH) and protionamide (PTH) that target mycolic acid biosynthesis (through inhibition of InhA).

1. Targeting InhA with fragment-based strategies

a. Boosting ETH and PTH bioactivation

Mycolic acid biosynthesis is achieved by the FAS-II pathway, responsible for the elongation of short mycolic acid precursors generated by the FAS-I system (Figure 1).[17] FAS-II enzymes (MabA (FabG1), HadAB/BC, KasA/B and InhA) are attractive drug targets since they are not present in eukaryotic cells. Among these, only InhA is targeted by the approved drugs ETH, PTH and INH, three prodrugs that require mycobacterial bioactivation[18] in order to generate covalent adducts with NAD^+ with very high affinities for InhA catalytic site.

The mycobacterial bioactivation of the two thioamide prodrugs ETH and PTH is performed by EthA and MymA, two flavin-dependent mycobacterial Baeyer-Villiger monooxygenases. This process is under the control of transcriptional repressors EthR.[19] For this reason, ETH and PTH are used with high doses in clinics as second line drugs because of the resulting very narrow therapeutic window. The therapeutic strategy consisting in inhibiting EthR has therefore emerged with the aim of potentiating the bioactivation of thioamides, and therefore their potency, thus making it possible to consider a reduction in therapeutic doses or at least to strengthen the effectiveness of the drug.

The first crystal structures of EthR serendipitously bound with hexyl octanoate [20] or 1,4-dioxane [21] revealed a conformation incompatible with DNA binding, which opened the way for structure-based design of EthR inhibitors[22] and the discovery of compounds that potentiate the activity of ethionamide *in vitro* but also *in vivo*[23].

In parallel, fragment-based approaches were also applied to discover new chemotypes of EthR inhibitors.[16, 24] This review will only focus on the most recent advances made in this field.

Starting from fragment **1** (ΔT_m (100 µM) = 3C, IC_{50} = 280 µM, EC_{50} = 3 µM), identified through a thermal-shift screen, Abell and co-workers developed fragment merging and linking approaches[25] to access compounds **2** and **3** respectively (Figure 2). These two optimized analogues showed a higher affinity for EthR than the initial hit, but were surprisingly found

less (or not) potent to boost ETH in macrophages infected *M.tb*. The authors attributed this lack of activity to poor membrane permeability of larger chemical structures. Therefore, starting from the same hit **1**, a third approach based on fragment-growing has recently been reported by Nikiforov *et al.*[26] Extensive exploration of structure-activity relationships was conducted by modifying the nature of the pyrrolidine ring, the nature of the amide linker, the length of the linear alkyl chain and the nature of the cyclopentyl ring in order to interact with residues Asn176 and Thr149. This led to compounds **4** and **5** (Figure 2) which displayed interesting EC_{50} of 0.4 µM. However, both compounds also shown intrinsic bactericidal activity (MIC_{50} = 1 µM).

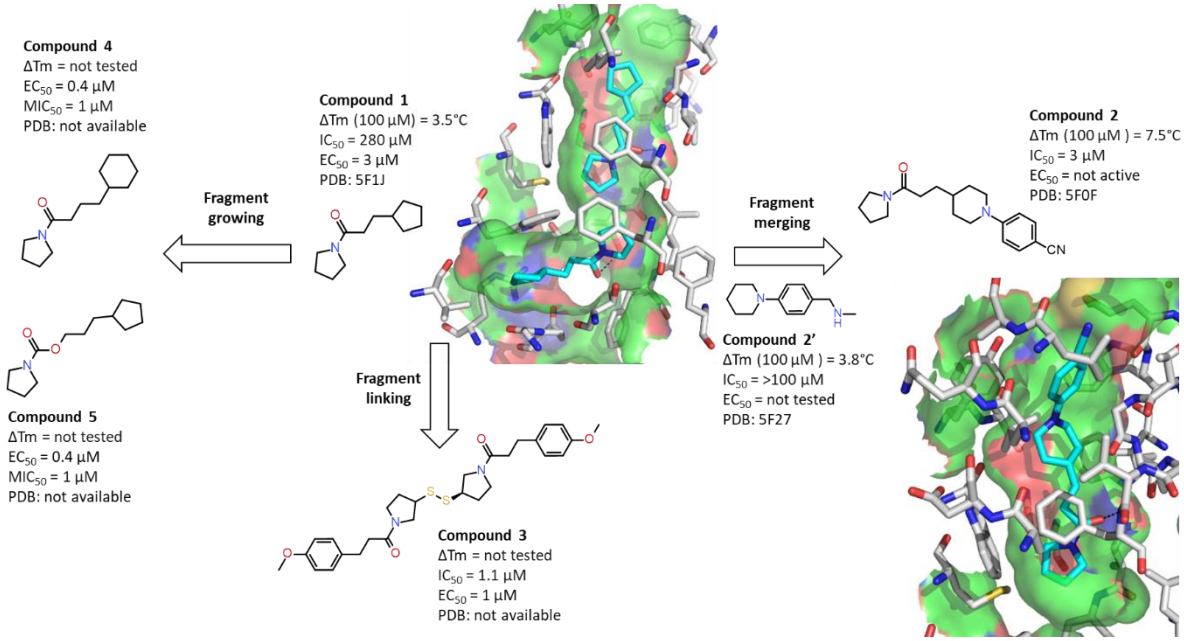

Figure 2 : Chemical structures and binding modes of EthR inhibitors optimized from fragment **1**, through fragment-merging, fragment-linking and fragment-growing approaches.[25, 26] Images generated with Pymol, hydrogen bonds shown as dashed-lines.

Villemagne *et al.*[27] came to the same conclusion that fragment-growing could lead to more potent and efficient ethionamide boosters very likely because of *M.tb* membrane permeability issues. Indeed, structure-guided optimization of fragment **6** (ΔT_m (20 µM) = 0.1°C, IC_{50} = 160 µM, EC_{50} > 20 µM) led to the nanomolar ETH booster **7** (ΔT_m (20 µM) = 11.2°C, IC_{50} = 0.4 µM, EC_{50} = 0.08 µM) (Figure 3). However, **7** was poorly stable in presence of mouse liver microsomes, and the main metabolism was found to happen through oxidation on the methyl moiety. Replacement of the metabolically fragile 2-methyl-1,3-thiazole moiety by a 2-cyclopropyl-1,2,4-oxadiazole led to compound **8** (ΔT_m (20 µM) = 10.2°C, EC_{50} = 0.07 µM, Cl_{int} = 69 $\mu L.min^{-1}.mg^{-1}$) with similar potency but improved ADME properties, suitable for *in vivo* evaluation (Figure 3). Noteworthily, administration via endotracheal route of polymeric cyclodextrin nanoparticles co-loaded with ETH + compound **8** in *M.tb* infected mice led to a 2 log units reduction of the pulmonary bacterial load, compared to the untreated group, and more than 1 log compared to the administration of ETH alone.[28] This

represents the first example of fragment-based EthR inhibitors with *in vivo* ethionamide boosting efficacy.

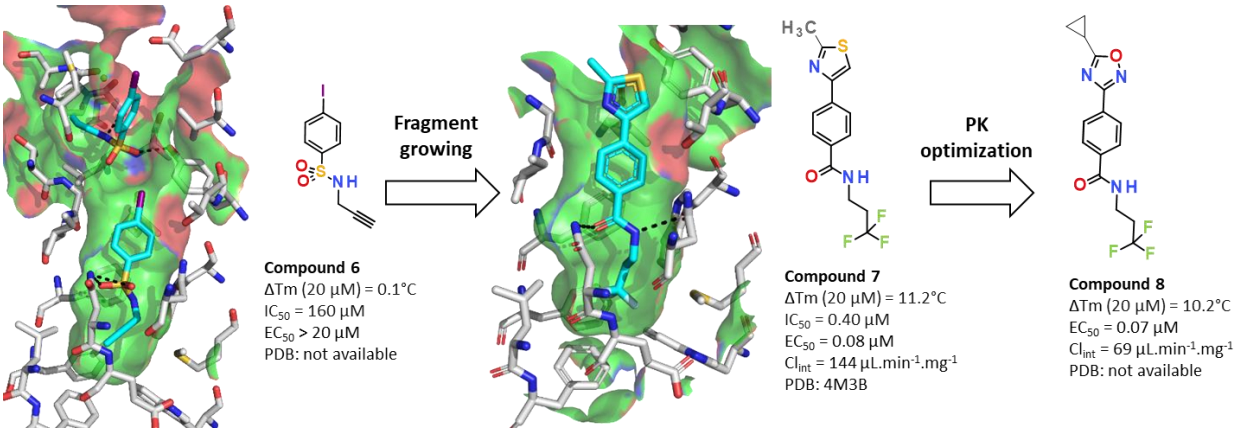

Figure 3 : Chemical structures and binding modes of EthR inhibitors optimized from fragment **6**, through fragment-growing approaches.[27, 28] Images generated with Pymol, hydrogen bonds shown as dashed-lines.

Unfortunately, boosting the bioactivation of ETH through overexpression of *ethA* will only impact *M.tb* strains sensitive to ETH, but not EthA-muted resistant strains. However, in the course of chemical exploration for EthR inhibitors, Blondiaux *et al.*[29] identified SMARt-420, a spiroisoxazoline based compound devoid of EthR affinity but still able of potentiating ETH activity. This discrepancy allowed for the identification of a second bioactivation pathway where the inhibition of a new transcriptional repressor, called $EthR_2$, by SMARt-420, leads to the expression of the oxidoreductase $EthA_2$, allowing for the thioamide prodrugs to be boosted in both ETH-sensitive and ETH-resistant strains.

Prevet *et al.*[30] described a fragment approach for the discovery of new chemical scaffold of $EthR_2$ inhibitors. A 960-fragment library was screened at 1 mM on $EthR_2$ using thermal shift assay (TSA), leading to 50 hits with a thermal stabilization (ΔT_m) higher than 1°C. Twelve of them were confirmed in a dose-response experiment (hit rate of 1.25 %) and were engaged in co-crystallization studies, leading to five resolved co-crystal structures. Fragment **9** had the highest affinity for $EthR_2$ (ΔT_m (1 mM) = 3.4°C). It was also able to disrupt the interaction between $EthR_2$ and its DNA-operator (IC_{50} = 1 µM). Fragment **9** occupies the same binding pocket as SMARt-420 (Figure 4). The tropane ring makes hydrophobic contacts with Trp100, Ala130 and Ile113 while the tertiary amine being forms a salt bridge with Asp168. The chlorophenyl moiety points towards the hydrophobic entrance of the binding domain. Structure-activity relationships were first explored by modifying the ethylene linker and the tropinone ring. All modifications led to less active compounds. The authors then focused on substitutions of the phenyl ring. The para-trifluoromethyl substituted compound **10** (ΔT_m (20 µM) = 0.6°C; IC_{50} = 0.2 µM) was found to have a similar binding mode as **9**, higher affinity for $EthR_2$ and be more potent at disrupting $EthR_2$-DNA interaction than hit compound **9**. Unfortunately, no boosting effect could be observed on *M.tb*.

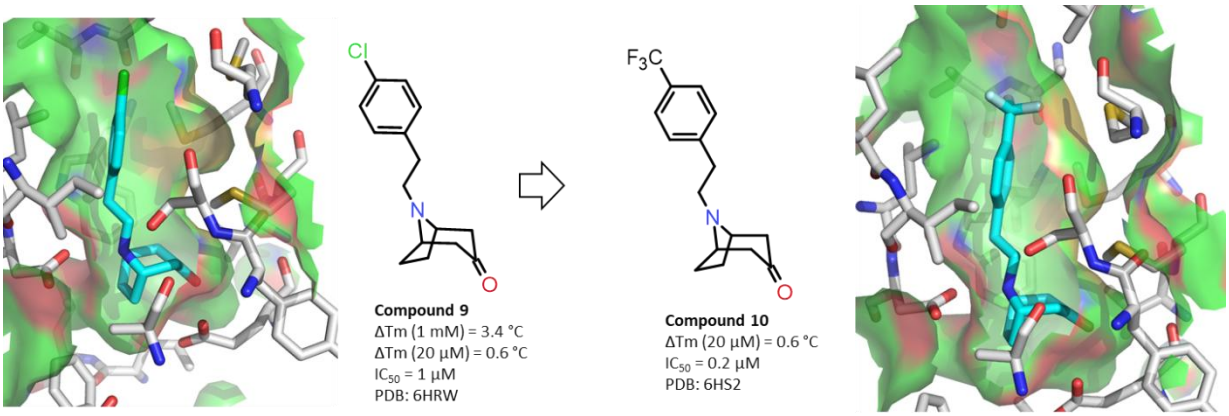

Figure 4 : Chemical structures and binding modes of EthR2 inhibitors optimized from fragment **9**, through fragment-growing approaches.[30] Images generated with Pymol.

Another conceivable strategy is the design of direct inhibitors of InhA that do not require bioactivation, and would therefore have no cross-resistance issues.[31] This has led to the discovery and development of several classes of inhibitors with very diverse structures coming from various approaches.[31] However, the first inhibitors coming from fragment-based approaches have only been reported very recently.

b. Direct inhibition of InhA with fragments

First, in 2018, Prati *et al.*[32] described the screening of a 1360-fragment library assembled from commercial libraries, commercial fragments from known InhA inhibitors, in-house fragments and a library of fragments specifically designed with derivatization moieties, so called "functional group complexity" (FGC) library. Pools of 8 fragments were screened against InhA using STD NMR (each fragment tested at a concentration of 0.5 mM), leading to 149 hits (hit rate 11%). Literature suggests that strong InhA inhibitors decrease the STD signals of the NADH cofactor, therefore, the 32 fragments able to do so were prioritized. In parallel, screening of the 149 initial fragments in a biochemical assay at a concentration of 0.5 mM only gave 4 hits, which were also part of the 32 strong binders able to decrease the NADH STD signal. 15 fragments were engaged in crystallography studies, leading to five resolved co-crystal structures. Strikingly, fragments **11** ($pIC_{50} < 3$) and **12** ($pIC_{50} < 3$) form a hydrogen-bond with the side chain of Tyr158 and the NADH ribosyl-20-OH moiety, a feature shared with the known InhA inhibitor **13** ($pIC_{50} = 5.0$) (Figure 5). On top of this key interaction, the pyrimidine ring of **11** interacts with the backbone NH of Met98, while the pyridine nitrogen of **12** is predicted to be protonated and interact with the side chain of Glu219. Overlay of the binding poses of **11**, **12** and **13**, allowed for the implementation of several fragment-merging strategies. For instance, fragments **11** and **12**, both inactive in the biochemical assay, were successfully merged into compound **14** ($pIC_{50} = 4.1$). The crystal structure of compound **14** bound to InhA reveals that the merge compound displays the binding features of the individual fragments. Adding a "magic methyl" in position 5 of the pyridine ring caused a ten-fold potency improvement (compound **15**, $pIC_{50} = 5.0$, $pK_d = 4.7$).

In parallel, including structural features of fragment **11** in the structure of the known InhA inhibitor **13** led to 1.5 log unit improvement in potency (compound **16**, pIC_{50} = 6.5).

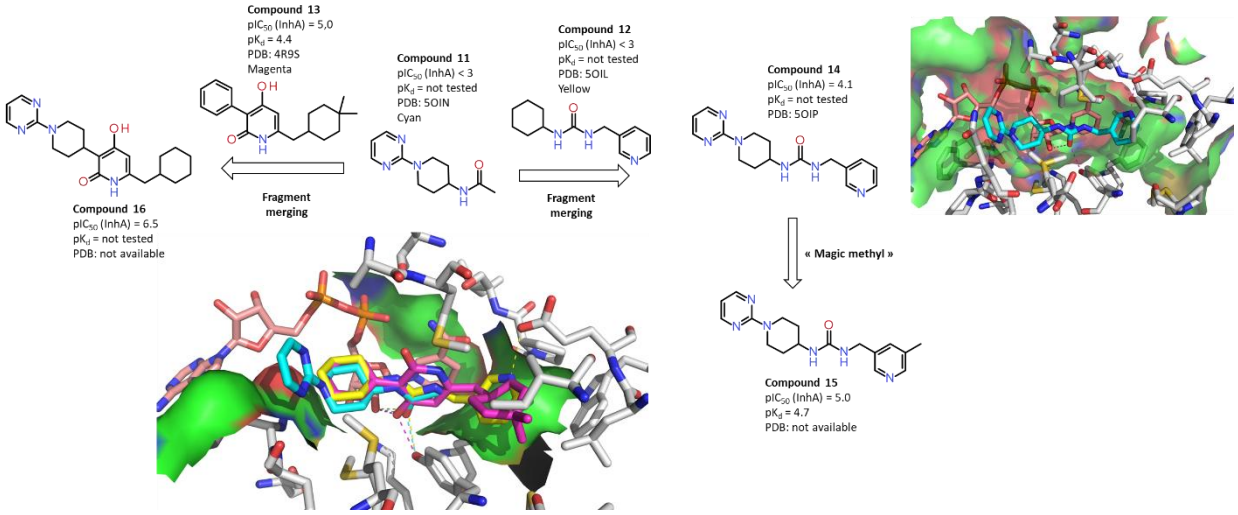

Figure 5 : Chemical structures and binding modes of InhA inhibitors optimized from fragment **11**, through fragment-merging approaches.[32] Images generated with Pymol, hydrogen bonds shown as dashed-lines.

Two other hits, fragments **17** and **18** were found to also form an hydrogen bond with the NADH ribosyl-20-OH moiety through the 2-N-pyrazole, but not with the Tyr185, since the side chain of the tyrosine is flipped. Not surprisingly, good overlay was observed between the binding mode of fragment **17** and **18**, and the 2 pyrazole containing inhibitors from the literature **19** and **20**. Therefore, another fragment-merging approach was considered. However, in this case, the newly designed analogs (compounds **21** and **22**) were less potent than compounds **19** and **20**.

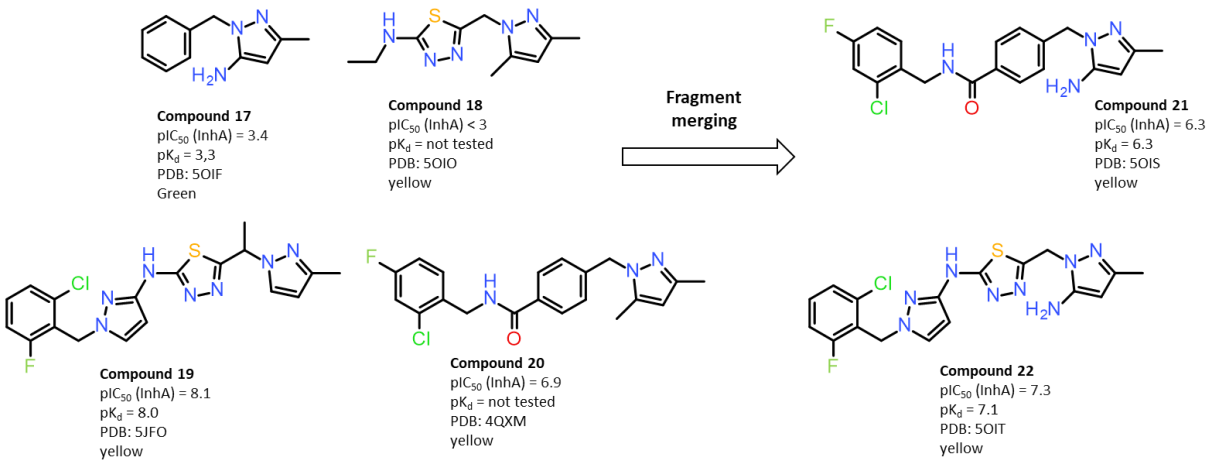

Figure 6: Chemical structures and optimisation of InhA inhibitors starting from fragment **17** and **18**.[32]

Sabbah *et al.*[33] used TSA to screen an in-house library of 800 rule-of-three compliant fragments. In order to find allosteric inhibitors that would not bind to the NAD binding

domain, the screening was performed in presence of a saturating concentration of NAD^+ (1 mM). 42 hits with a $\Delta T_m \geq 3°C$ (hit rate of 5.2%) were identified. They were then further confirmed using three different ligand-based NMR techniques: CPMG, WaterLOGSY and STD. 18 fragments were confirmed in at least two of the three NMR experiments. Interestingly, 15 of them displayed a carboxylic acid moiety. All 18 fragments were soaked into InhA crystals at 20 mM, yielding 5 well-defined crystal structures. The authors selected fragment **23** as a starting point for optimization based on chemical scaffold novelty (Figure 7). The carboxylic acid of **23** is interacting with the side chain of Tyr158 as well as the ribose ring from the cofactor. Overlaying the binding mode of triclosan, a known inhibitor of InhA, with fragment **23** highlighted that the carboxylic acid of **23** occupies the same region as the ether linker from triclosan. The authors therefore decided to replace the carboxylic acid moiety by a sulfonamide and use it as a vector to further explore the InhA pocket, leading to the merged compound **24** with a significantly improved activity (54% of InhA inhibition at 0.1 mM) compared to fragment **23** (no inhibition of InhA at 2 mM). Structure-activity relationships were then explored around the freshly added phenyl ring, by changing the nature of the ring or adding various substituents. Introduction of a methylamine moiety in meta position of the phenyl ring (compound **25**, IC_{50} = 4 µM) led to a drastic increase in potency. Docking studies suggested that a hydrogen-bond between the nitrogen of the methylamine and the phosphate of NAD^+ could be responsible of this increase in potency. Finally, cyclizing the molecule to get rid of the potentially metabolically unstable styrene motif led to sub-micromolar analog compound **26** (IC_{50} = 0.31 µM). The X-ray analysis of the InhA-**26** complex (Figure 7) confirmed the predicted interactions between the sulfonamide and Tyr158 on one hand and between the methylamine and the phosphate of NAD^+ on the other hand. However, compound **26** was not able to decrease the production of mycolic acids and was inactive against *M.tb*. The researchers suggest that this could be due to insufficient cell permeability, drug efflux or drug metabolism.

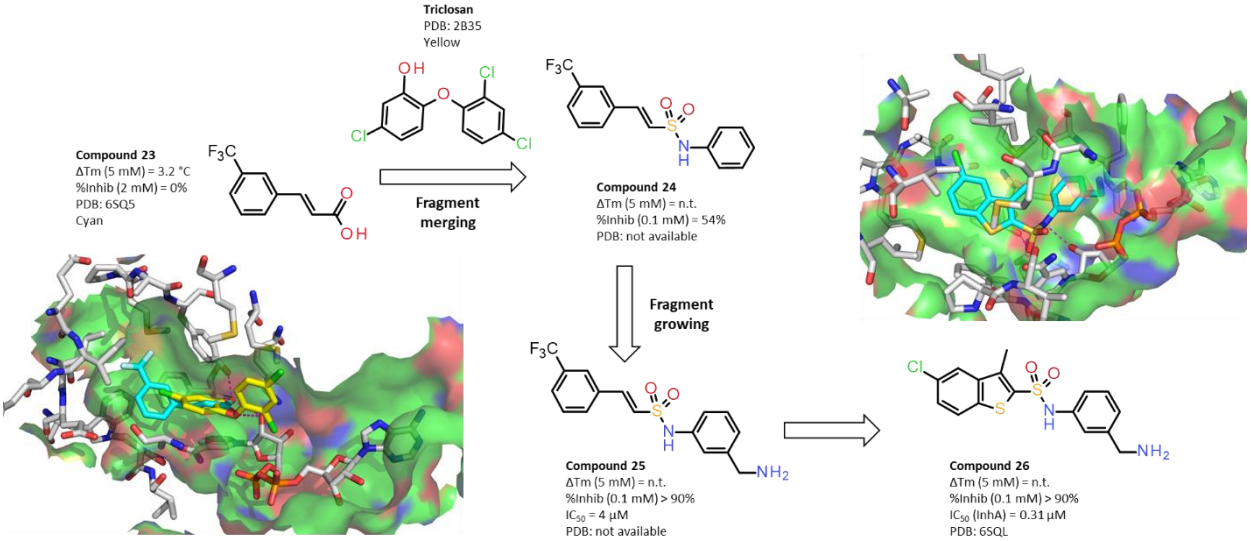

Figure 7 : Chemical structures and binding modes of InhA inhibitors optimized from fragment **23**, through fragment-merging approaches.[34] Images generated with Pymol, hydrogen bonds shown as dashed-lines.

All the fragment-based families previously described either directly inhibit InhA or boost the bacterial bioconversion of prodrugs into InhA inhibitors. In addition to InhA, three other enzymes are involved in the FAS-II system in charge of the elongation of mycolic acids: FabH, MabA (FabG1) and HadAB/BC.[35] Among all these essential enzymes, only MabA does not have any specific inhibitors.

2. Targeting FabG1 with fragment-based strategies

Faion *et al.*[36] implemented a fragment-based approach for the discovery of the first specific inhibitors of MabA. A 1280 fragments library assembled with commercially available fragments and sp^3-enriched synthetic molecules[37], was screened at 1 mM using an LCMS/MS-based enzymatic assay. 50 hits with a percentage of inhibition higher than 30% were identified among which 12 were confirmed in dose-response experiments with IC_{50} lower than 300 µM. 68 commercially available analogs of the 12 hits were also tested and led to the selection of 6 chemical series. Since only the anthranilic acid family (represented by compound **27,** Figure 8) displayed antibacterial activity (MIC_{90} = 300 µM), it was selected for further optimization. Neither modification of the carboxylic acid moiety, nor substitution of positions 4 and 5 of the phenyl ring led to an improvement of the activity. However, the carbamate moiety was advantageously replaced by an amide. Structural exploration of the amide substituent led to compound **28** with a 3,4-dichlorophenyl moiety (Figure 8) (IC_{50} = 38 µM, MIC = 300 µM). Compound **28** was found to be seven times more active than compound **27** in the enzymatic assay but surprisingly did not show any improved antimycobacterial activity. Despite the fact that affinities of fluorinated analogs of compound **28** for MabA (evaluated by ^{19}F-NMR) correlated well with enzymatic IC_{50}, the authors do not exclude the fact that the observed antimycobacterial activity could be due to another mechanism of action.

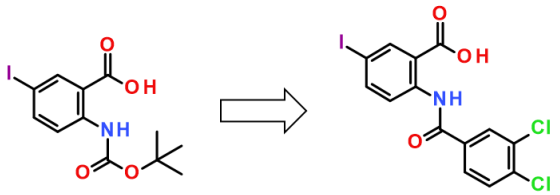

Compound 27
IC_{50} = 280 µM
MIC_{H37Rv} = 300 µM

Compound 28
IC_{50} = 38 µM
MIC_{H37Rv} = 300 µM

Figure 8 : Chemical structures of MabA inhibitors optimized from fragment 27, through fragment-approach approaches.[36]

Among the five FabG genes encoded in the *M.tb* genome, only FabG1 (Rv1483) and FabG4 (Rv0242c) are conserved among all mycobacterial species.[38] Just like FabG1, FabG4 was shown to be essential for bacterial growth.[39]

3. Targeting FabG4 with fragment-based strategies

Starting with the crystal structure of NADH-bound FabG4, Banerjee *et al.*[40] used computational fragment-based drug design the first inhibitors of FabG4. To this purpose

they gathered fragments and linkers from the literature and merged them to form a library of potential FabG inhibitors. Since several polyphenol derivatives have been shown to be FabG inhibitors[41], they included polyphenols in the fragment-based library. With the aim of targeting the NADH-binding site, they included 1,4-triazole linkers in the linker library since Chen *et al.*[42] demonstrated that 1,4-triazoles can be used as bioisosters of the pyrophosphate linker of NADH, one of FabG4 substrate. The authors selected diastereoisomers **29** and **30** as putative FabG4 inhibitors (Figure 9). Interestingly, the trans stereoisomer **30** (IC_{50} = 35 µM, MIC = 5 $\mu g.mL^{-1}$) was found more active than the cis stereoisomer **29** (IC_{50} = 45 µM, MIC = 20 $\mu g.mL^{-1}$) both in the FabG4 enzymatic assay and in the *M. smegmatis* growth inhibition assay. Docking studies suggested that the triazole linker binds in the pyrophosphate binding pocket, as expected. Moreover, compounds **29** and **30** both are predicted to compete, as targeted, with the NADH binding domain and interact with FabG4 through many H-bonds. While compound **29** seems to interact with the nicotinamide binding subsite (N-subsite), the adenosine binding subsite (A-subsite) and the pyrophosphate binding subsite, compound **30** does not show any interaction with the A-subsite and seems to interact instead with the acetoacetyl CoA sub-domain. This could explain why compound **29** was found to be a competitive inhibitor of FabG4 (with respect to NADH) while mixed type of inhibition was observed for compound **30**. However, the binding energies measured in the docking study do not correlate with the measured Ki and IC_{50}. Replacing the catechin moiety with a m-cresol unit (Figure 9) led to the inactive analog **31** (IC_{50} = >400 µM). Removing the hydroxyl groups of the gallol moiety also decreases the affinity for FabG4 (compound **32**, IC_{50} = 213 µM).

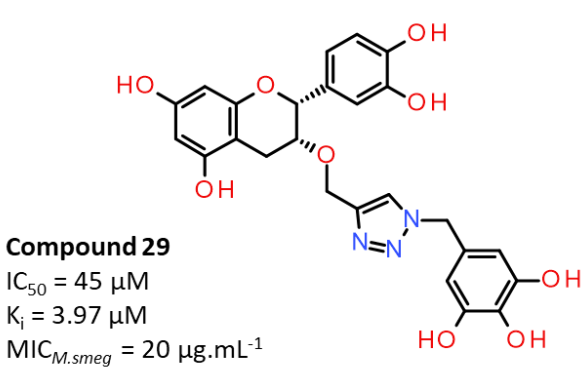

Compound 29
IC_{50} = 45 µM
K_i = 3.97 µM
$MIC_{M.smeg}$ = 20 µg.mL^{-1}

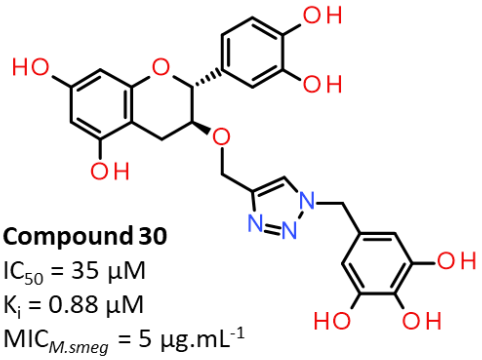

Compound 30
IC_{50} = 35 µM
K_i = 0.88 µM
$MIC_{M.smeg}$ = 5 µg.mL^{-1}

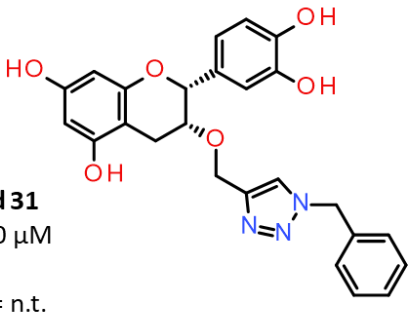

Compound 31
IC_{50} = > 400 µM
K_i = n.t.
$MIC_{M.smeg}$ = n.t.

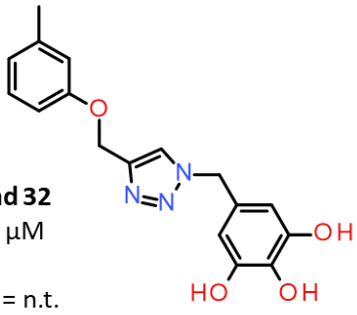

Compound 32
IC_{50} = 213 µM
K_i = n.t.
$MIC_{M.smeg}$ = n.t.

Figure 9 : Chemical structures of FabG4 inhibitors derived from *in silico* screening.[40]

Development of Fragments targeting metabolites synthesis

1. Targeting *Mt*DHFR with fragments

Dihydrofolate reductase (DHFR) is a key enzyme for mammals as well as microorganisms such as *M. tb*. Indeed, it is responsible for the biosynthesis of tetrahydrofolic acid which is required for the biosynthesis of purine and thymidine nucleotides along with many amino acids.[43] Several approaches have been developed for the discovery of promising *Mycobacterium tuberculosis* Dihydrofolate reductase (*Mt*DHFR) inhibitors but none of them has reached clinical trials yet. Shelke *et al.*[44] have used virtual screening for the identification of new chemotypes of *Mt*DHFR inhibitors. They used a rule of three compliant virtual library of heterocycle-based fragments and identified several scaffolds. All the fragments identified showed hydrogen bonding with the backbone of Ile94 and some of them also interacted with Asp27 and Phe31. These binding modes have not been confirmed by X-ray crystallography yet. 20 hits were synthesized and screened against *Mt*DHFR to measure IC_{50} but also against *M. tb* H37Rv to determine MIC. All compounds showed activity against *Mt*DHFR (IC_{50} ranging from 39 to 90 µM) but only compounds with a quinazolin-4-one moiety, mimicking tetrahydrofolate, (such as compound **33**, ***Figure 10***) had MIC below 125 µg/mL (ranging from to 31.5 to 125 µg/mL). No correlation could be observed between IC_{50} and MIC.

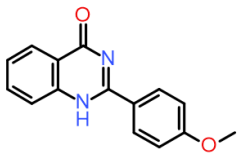

Compound 33
IC_{50} (*Mt*DHFR) = 49 µM
MIC (H37Rv) = 32 µg.mL^{-1}

Figure 10 : Chemical structures of a representative inhibitor of MtDHFR derived from *in silico* screening.[44]

Ribeiro *et al.*[45] screened a rule of three compliant library of 1250 fragments against *Mt*DHFR using TSA. This led to the identification of 37 compounds with a $\Delta T_m \geq 0.5$ °C (hit rate 2.8%). Interestingly, most of the compounds display a carboxylic acid moiety hold by an aromatic ring. 1D STD-NMR was used as a secondary screening to confirm 21 fragments and highlighted the importance of the benzoic acid moiety for the binding with the protein. The fragments were further confirmed by ITC, which led to the selection of 8 fragments with Kd ranging from 0.095 to 3.2 mM. Interestingly, except for compound **34** (***Figure 11***), all the other fragments showed unique site occupancy. This was confirmed by the X-ray analysis of *Mt*DHFR complexes with the fragments. Indeed, compound **34** was found to simultaneously bind to the entrance pocket through an ionic interaction with the side chain of Arg60, as most of the identified fragments, but was the only one to also interact with the glycerol binding pocket through a hydrogen bond with the side chain of Gln28. Because this glycerol binding pocket can be found in *Mt*DHFR but not in the human DHFR, the authors selected fragment **34** as starting point for optimisation. A fragment-growing approach was implemented, by substituting position 5 of the pyrazole ring, leading to compound **35** (ΔT_m = 5.1°C; Kd = 0.017 mM; LE = 0,24) with improved affinity for *Mt*DHFR but slightly decreased ligand efficiency. Analysis of *Mt*DHFR complex with compound **35** (***Figure 11***) indicates that the carboxylic acid moiety retains the ionic interaction with Arg60 at the entrance pocket while the oxygen of the newly introduced propenamide linker forms a hydrogen-bond with Gln28, replacing the second unit of compound **34**.

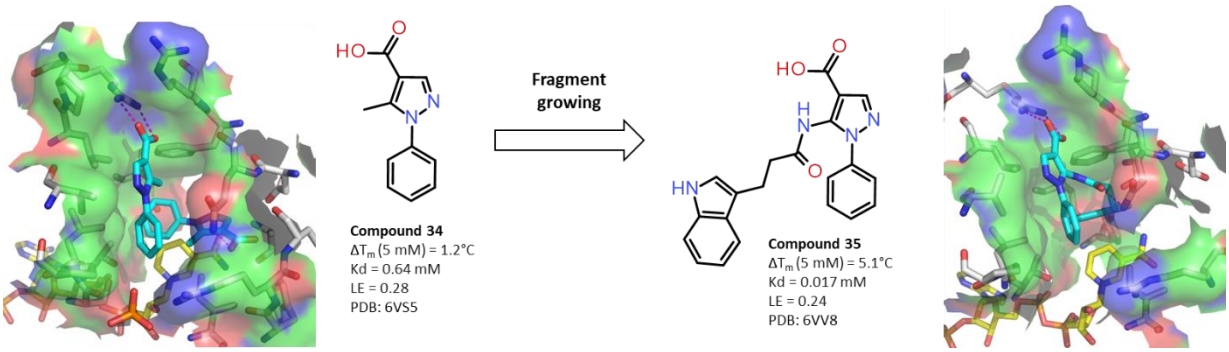

Figure 11 : Chemical structures and binding modes of MtDHFR inhibitors optimized from fragment 34, through a fragment-growing approach.[45] Images generated with Pymol, hydrogen bonds shown as dashed-lines.

2. Targeting IMPDH with fragments

Another enzyme involved in the biosynthesis of nucleotides has received more and more attention in the last two decades: inosine-5'-monophosphate dehydrogenase (IMPDH). This

enzyme oxidizes inosine 5'-monophopshate (IMP) into xanthosine 5'-monophosphate (XMP), which is then converted to guanosine 5'-monophosphate. IMPDH has been showed essential for many pathogens including *M. tb*, and therefore there has considerable efforts made in the last 10 years in order to identify of IMPDH inhibitors as potential new drug candidates. Trapero *et al.*[46] have recently reported fragment-linking and fragment-merging approaches for the discovery of new chemotypes of IMPDH inhibitors. They used IMPDH from *Mycobacterium thermoresistible* (*M. th*) as a model because it shares 100% identity with *M. tb* IMPDH in the active site, and is easier to produce and crystallize. A 960 fragments library was screened at 1 mM using a biochemical assay leading to 18 hits with a percentage of inhibition higher than 50% (1.9 % hit rate). IC_{50} were measured for six of them, ranging from 325 µM to 674 µM (LE ranging from 0.31 to 0.42). The binding mode of these six fragments was elucidated using X-ray crystallography by soaking with *M. th* IMPDH. Although it was the weakest of the six hits, electron density could only be observed for fragment **36** (IC_{50} = 674 µM, LE = 0.36). **36** was able to bind two times simultaneously within the NAD binding pocket (***Figure 12***): The first one is π-stacked with the hypoxanthine of IMP and makes polar contact with Gly318 and Glu442 while the second one is hydrogen bonded with Glu442. The authors therefore considered both fragment-growing and fragment-linking for the optimization **36**. Interestingly the phenyl ring of the IMP π-stacked fragment **36** and the imidazole ring of the second fragment **36** unit overlap well with the phenyl rings of the previously described IMPDH inhibitor **37**.[47] They thus decided to use the lactate linker found in compound **37** to link the 2 units of **36**, leading to the 2500-fold more potent but less efficient compound **38** (IC_{50} = 0.27 µM, LE = 0.30). The other tested linkers were found to be less attractive.

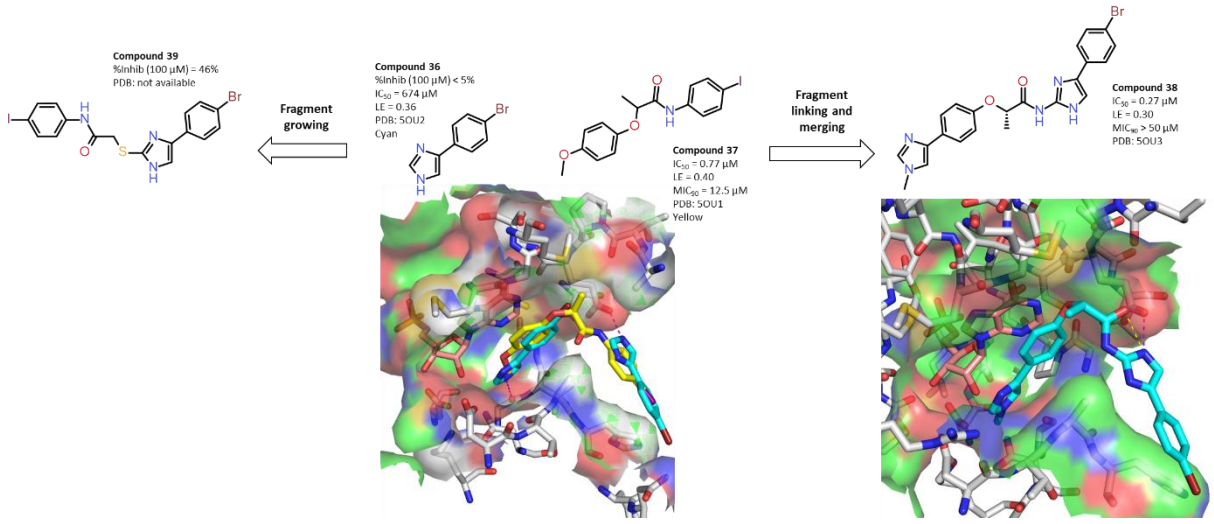

Figure 12 : Chemical structures and binding modes of IMPDH inhibitors optimized from fragment 36, through a fragment-linking and fragment-merging approach.[45] Images generated with Pymol, hydrogen bonds shown as dashed-lines.

X-ray analysis of IMPDH crystals soaked with compound **38** showed not only it retains the key interactions formed by fragment **36** and lead **37** but also creates additional polar contacts with Asp267 and Asn297. Despite these various interactions, compound **38** suffered severe ligand efficiency drop compared to fragment **36** and compound **37**. Moreover, no

significant inhibition of bacterial growth could be observed at concentrations up to 50 µM, unlike compound **37** (MIC_{90} = 12.5 µM). The authors are currently investigating a potential membrane permeability issue or drug-efflux mechanisms.

In parallel to this fragment-linking/merging approach, a fragment-growing approach was used by the extension of fragment **36** at position 2 of the imidazole ring. They mainly substituted this position with various aromatic rings linked by a thioacetamide, a motif found in previously described IMPDH inhibitors. Although the activity of fragment **36** (<5% inhibition @100 µM) could be improved (***Figure 12***, compound **39**; 46% inhibition @100 µM), all the analogues from the fragment-growing approach were found to be less active than the merged analog **38**.

3. Targeting GlcB with fragments

The glyoxylate shunt plays an important role in *M.tb* virulence. It consists of the hydrolysis of isocitrate into glyoxylate and succinate by the isocitrate lyase (ICL), followed by the conversion of glyoxylate into malate by the malate synthase (GlcB). Huang *et al.* [48] used TSA to screen the affinity of 1580 fragments for GlcB. 65 hits with a ΔT_m higher than 3°C were selected for co-crystallization experiment, leading to 18 complex structures. Interestingly, 16 of them displayed a carboxylic acid function that chelates the Mg^{2+} ion, a feature shared with the known inhibitors from the phenyldiketo acids family (PDKA, compound **40** for instance)[49]. The fragments were then separated in two groups based on the conformation of the protein induced upon ligand binding. Noteworthily, 8 out of the 13 fragments in group 2 displayed H-bonding with the backbone carbonyl of Met631 through a nitrogen involved in an aromatic system. The authors therefore decided to introduce the hydrogen bond forming potential of these fragments in the previously described PDKA inhibitors. This resulted in indole-based diketo acid compounds among which compound **41** (***Figure 13***) was the most active (IC_{50} = 0.02 µM). The N-methylated analog was found to be 100-fold less active than its counterpart, suggesting the importance of the hydrogen-bond donor potential of the indole nitrogen. This was confirmed by co-crystallization of compound **41**, revealing H-bond with the backbone of Met631. Interestingly, compound **41** was more potent against GlcB than the original PKDA compound **40**, but no activity on *M. tb* has been reported for this compound.

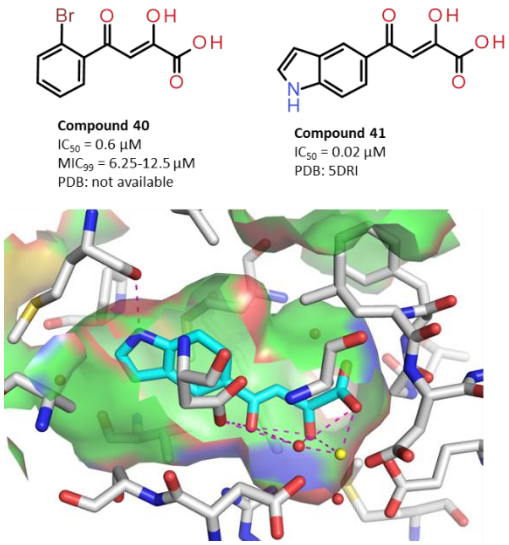

Figure 13 : Chemical structures and binding modes of GlcB inhibitor 41 optimized through fragment-merging approach.[48] Images generated with Pymol, hydrogen bonds shown as dashed-lines.

Development of Fragments targeting host-pathogen interactions

In the last decades, more and more attention has also been dedicated to host-pathogen interactions for the discovery of new drug targets.[50] In particular, it has been shown that host cholesterol plays an important role in the infection process[51] and can be used as a carbon source inside the macrophages.[52] It has previously been demonstrated that HsaC and HsaD, two enzymes from the superfamily of α/β-hydrolases, have been proven essential for the survival of *M.tb* within macrophages.[53] HsaD cleaves carbon-carbon bonds through a serine-protease catalytic triad in the cholesterol metabolism pathway. Ryan *et al.*[54] have recently described a fragment-based approach for the discovery of the first HsaD inhibitors. Screening of a 1258 fragments library by TSA led to the identification of 18 hits (1.4% hit rate) which were then tested by TSA, leading to 8 reconfirmed fragments. The validated hits were then evaluated in a biochemical assay for their ability to inhibit HsaD at a concentration of 1 mM and by STD NMR for their ability to displace phenylmethylsulfonyl fluoride (PMSF), a non-specific and covalent inhibitor from the literature.[55] These successive steps allowed for the identification of 7 fragments able to bind HsaD, among which 5 were able to displace PMSF. Sulfonamide fragment **42** (IC_{50} = 0.41 mM; MIC (*M. tb*) = 25 $\mu g.mL^{-1}$; MIC (*M. bovis* BCG) < 12.5 $\mu g.mL^{-1}$) and hydroxybenzoate fragment **43** (IC_{50} = 0.52 mM; MIC (*M. tb*) < 12.5 $\mu g.mL^{-1}$; MIC (*M. bovis* BCG) < 12.5 $\mu g.mL^{-1}$) were the most promising (**Figure 14**), and were therefore selected for structure-activity relationship exploration. Displacing or removing the chlorine atoms from fragment **42** led to a loss of potency. Similar results were observed when replacing them with various substituents. Potency in the HsaD inhibition assay could be improved by introducing an amino moiety in position 4 (compound **44**, IC_{50} = 0.16 mM, **Figure 14**). However, this led to a decreased potency on *M. tb* growth inhibition (MIC (*M. tb*) = 200 $\mu g.mL^{-1}$). Similarly, replacing, removing or displacing the chlorine atoms in compound **44** led to a significant drop in potency. The hydroxyl group was found to be

essential and could only be replaced by an amino group. The ethyl ester could be replaced by a carboxylic acid moiety (compound **45**, IC_{50} = 0.54 mM, Figure 13) without altering the HsaD inhibitory potency, but with a loss in terms of *M. tb* growth inhibition (MIC = 200 $\mu g.mL^{-1}$). These fragments were found to be non-cytotoxic, and not active against *E.coli* at concentrations up to 100 $\mu g.mL^{-1}$, and therefore represent an interesting starting points for the development of new selective *M. tb* inhibitors by fragment-growing, through the use of the available co-crystal structures.

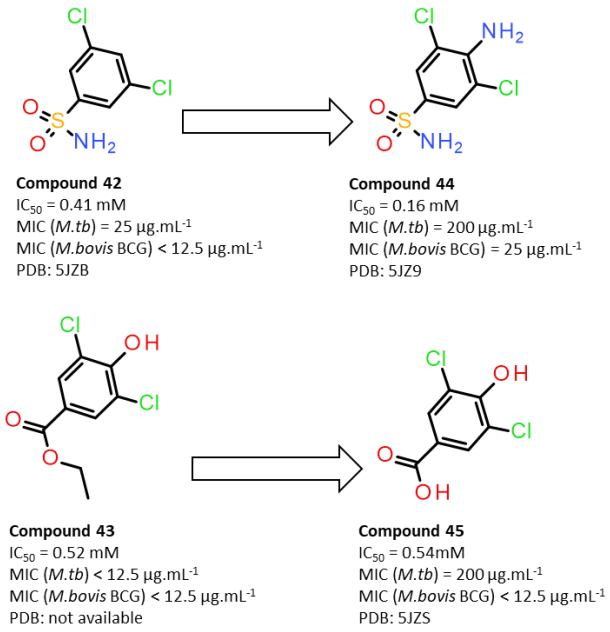

Compound 42
IC_{50} = 0.41 mM
MIC (*M.tb*) = 25 $\mu g.mL^{-1}$
MIC (*M.bovis* BCG) < 12.5 $\mu g.mL^{-1}$
PDB: 5JZB

Compound 44
IC_{50} = 0.16 mM
MIC (*M.tb*) = 200 $\mu g.mL^{-1}$
MIC (*M.bovis* BCG) = 25 $\mu g.mL^{-1}$
PDB: 5JZ9

Compound 43
IC_{50} = 0.52 mM
MIC (*M.tb*) < 12.5 $\mu g.mL^{-1}$
MIC (*M.bovis* BCG) < 12.5 $\mu g.mL^{-1}$
PDB: not available

Compound 45
IC_{50} = 0.54mM
MIC (*M.tb*) = 200 $\mu g.mL^{-1}$
MIC (*M.bovis* BCG) < 12.5 $\mu g.mL^{-1}$
PDB: 5JZS

Figure 14: Chemical structures of HsaD inhibitors 42-45 identified by fragment screening.[54]

Phenotypic-screening based approaches

In many of successful hit-to-lead optimization examples described hereabove, we have seen that strong "on-target" potency does not necessarily transpose into anti-mycobacterial activity. These examples illustrate a problem which has now been highlighted many times for more than one decade.[56, 57] As already mentioned, the main reason for this high attrition rate is the thick, complex and poorly permeable mycobacterial cell-wall, preventing many lead compounds from entering the mycobacterial fortress. This envelop is also very poorly permeable to drug-like molecules found in screening libraries, which usually results in very poor hit rates [56, 58]. Small and moderately lipophilic molecules are more likely to be able to cross the mycobacterial envelop and reach their target. Thereby, fragments seem particularly well-suited for phenotypic whole-cell screening. Moreira *et al.* [59] have screened an assembled library of 1725 commercially available fragments at 500 µM against *M. bovis* BCG as a *M. tb* surrogate. 116 hits were selected with a growth inhibition higher than 80%

and were then tested for growth inhibition of *M. tb* in a dose-response experiment, resulting in 38 hits with MIC_{50} < 500 µM. Interestingly, the compounds were found to be quite specific to mycobacteria, with 23 hits being also active against *M. avium* and 13 of them being active against *M. abscessus*, while most compounds were found inactive against a panel of fungi, gram positive and gram-negative bacteria. However, it should be noted that more than half of the fragments were also found toxic for HepG2 cells with selectivity indexes lower than 5. Many current anti-Tb drugs are pro-drug fragments, which require mycobacterial bioactivation into their active form. Whether the 38 hits identified in this screening are prodrugs or not is currently being investigated by the authors.

Conclusion

In the last two decades, fragment-based approaches have emerged as a powerful complementary tool for the discovery of new bioactive molecules, leading to four FDA approved drugs and dozens of clinical candidates. In the TB field, as we just saw, FBDD has been used more and more extensively for the discovery of hits against so far undruggable targets or the discovery of new chemotypes against known targets. However, this has not led to promising candidates yet. Indeed, many of the optimized hit compounds reviewed hereabove were found very potent in target-based assays but failed to show activity against *M. tb* and only one compound (EthR inhibitor) displayed *in vivo* activity. This can be explained by the fact that crystallography is a crucial factor for the success of FBBD approaches which have always been highly centered on target-based assays. Therefore, the cell permeability is evaluated and optimized at a later stage, which has been proven challenging. We think that the use of fragment-based approaches should engage a shift to whole-cell screenings as has been observed in the last decade in the TB drug discovery field. Many fragment sized molecules have been used for the treatment of tuberculosis, most of them being prodrugs. On top of allowing for the discovery of cell-permeable compounds, whole-cell screening of fragments could also allow for the discovery of new fragment prodrugs.[14] Overall, more chemistry is required in order to explore the chemical space further and lay the foundations of successful future screenings.

(1) WHO. *2020 Global Tuberculosis Report*; 2020.
(2) WHO. *2021 Global Tuberculosis Report*; 2021.
(3) Andries, K.; Verhasselt, P.; Guillemont, J.; Gohlmann, H. W.; Neefs, J. M.; Winkler, H.; Van Gestel, J.; Timmerman, P.; Zhu, M.; Lee, E.; et al. A diarylquinoline drug active on the ATP synthase of Mycobacterium tuberculosis. *Science (New York, N.Y.)* **2005**, *307* (5707), 223-227. DOI: 10.1126/science.1106753 From NLM.
(4) Palmer, B. D.; Thompson, A. M.; Sutherland, H. S.; Blaser, A.; Kmentova, I.; Franzblau, S. G.; Wan, B.; Wang, Y.; Ma, Z.; Denny, W. A. Synthesis and Structure−Activity Studies of Biphenyl Analogues of the Tuberculosis Drug (6S)-2-Nitro-6-{[4-(trifluoromethoxy)benzyl]oxy}-6,7-dihydro-5H-imidazo[2,1-b][1,3]oxazine (PA-824). *Journal of Medicinal Chemistry* **2009**, *53* (1), 282-294. DOI: 10.1021/jm901207n. Sasaki, H.; Haraguchi, Y.; Itotani, M.; Kuroda, H.; Hashizume, H.; Tomishige, T.; Kawasaki, M.; Matsumoto, M.; Komatsu, M.; Tsubouchi, H. Synthesis and Antituberculosis Activity of a Novel Series of Optically Active 6-Nitro-2,3-dihydroimidazo[2,1-b]oxazoles. *Journal of Medicinal Chemistry* **2006**, *49* (26), 7854-7860. DOI: 10.1021/jm060957y.
(5) J Libardo, M. D.; Boshoff, H. I. M.; Barry, C. E. The present state of the tuberculosis drug development pipeline. *Current Opinion in Pharmacology* **2018**, *42*, 81-94. DOI: https://doi.org/10.1016/j.coph.2018.08.001. Tornheim, J. A.; Dooley, K. E. The Global Landscape of Tuberculosis Therapeutics. *Annual Review of Medicine* **2019**, *70* (1), 105-120. DOI: 10.1146/annurev-med-040717-051150 (acccessed 2020/06/09).
(6) Romasanta, A. K. S.; van der Sijde, P.; Hellsten, I.; Hubbard, R. E.; Keseru, G. M.; van Muijlwijk-Koezen, J.; de Esch, I. J. P. When fragments link: a bibliometric perspective on the development of fragment-based drug discovery. *Drug Discovery Today* **2018**, *23* (9), 1596-1609. DOI: https://doi.org/10.1016/j.drudis.2018.05.004.

(7) Hall, R. J.; Mortenson, P. N.; Murray, C. W. Efficient exploration of chemical space by fragment-based screening. *Progress in Biophysics and Molecular Biology* **2014**, *116* (2), 82-91. DOI: https://doi.org/10.1016/j.pbiomolbio.2014.09.007. Hann, M. M.; Leach, A. R.; Harper, G. Molecular Complexity and Its Impact on the Probability of Finding Leads for Drug Discovery. *Journal of Chemical Information and Computer Sciences* **2001**, *41* (3), 856-864. DOI: 10.1021/ci000403i.
(8) Hopkins, A. L.; Groom, C. R.; Alex, A. Ligand efficiency: a useful metric for lead selection. In *Drug Discov Today*, Vol. 9; 2004; pp 430-431.
(9) Waring, M. J.; Arrowsmith, J.; Leach, A. R.; Leeson, P. D.; Mandrell, S.; Owen, R. M.; Pairaudeau, G.; Pennie, W. D.; Pickett, S. D.; Wang, J.; et al. An analysis of the attrition of drug candidates from four major pharmaceutical companies. *Nature Reviews Drug Discovery* **2015**, *14* (7), 475-486. DOI: 10.1038/nrd4609.
(10) Kirsch, P.; Hartman, A. M.; Hirsch, A. K. H.; Empting, M. Concepts and Core Principles of Fragment-Based Drug Design. *Molecules* **2019**, *24* (23). DOI: 10.3390/molecules24234309. Osborne, J.; Panova, S.; Rapti, M.; Urushima, T.; Jhoti, H. Fragments: where are we now? *Biochem Soc Trans* **2020**, *48* (1), 271-280. DOI: 10.1042/bst20190694 From NLM.
(11) Bollag, G.; Tsai, J.; Zhang, J.; Zhang, C.; Ibrahim, P.; Nolop, K.; Hirth, P. Vemurafenib: the first drug approved for BRAF-mutant cancer. *Nature Reviews Drug Discovery* **2012**, *11* (11), 873-886. DOI: 10.1038/nrd3847. Souers, A. J.; Leverson, J. D.; Boghaert, E. R.; Ackler, S. L.; Catron, N. D.; Chen, J.; Dayton, B. D.; Ding, H.; Enschede, S. H.; Fairbrother, W. J.; et al. ABT-199, a potent and selective BCL-2 inhibitor, achieves antitumor activity while sparing platelets. *Nat Med* **2013**, *19* (2), 202-208. DOI: 10.1038/nm.3048 From NLM. Perera, T. P. S.; Jovcheva, E.; Mevellec, L.; Vialard, J.; De Lange, D.; Verhulst, T.; Paulussen, C.; Van De Ven, K.; King, P.; Freyne, E.; et al. Discovery and Pharmacological Characterization of JNJ-42756493 (Erdafitinib), a Functionally Selective Small-Molecule FGFR Family Inhibitor. *Mol Cancer Ther* **2017**, *16* (6), 1010-1020. DOI: 10.1158/1535-7163.mct-16-0589 From NLM. Tap, W. D.; Wainberg, Z. A.; Anthony, S. P.; Ibrahim, P. N.; Zhang, C.; Healey, J. H.; Chmielowski, B.; Staddon, A. P.; Cohn, A. L.; Shapiro, G. I.; et al. Structure-Guided Blockade of CSF1R Kinase in Tenosynovial Giant-Cell Tumor. *N Engl J Med* **2015**, *373* (5), 428-437. DOI: 10.1056/NEJMoa1411366 From NLM. Lanman, B. A.; Allen, J. R.; Allen, J. G.; Amegadzie, A. K.; Ashton, K. S.; Booker, S. K.; Chen, J. J.; Chen, N.; Frohn, M. J.; Goodman, G.; et al. Discovery of a Covalent Inhibitor of KRASG12C (AMG 510) for the Treatment of Solid Tumors. *Journal of Medicinal Chemistry* **2020**, *63* (1), 52-65. DOI: 10.1021/acs.jmedchem.9b01180. Schoepfer, J.; Jahnke, W.; Berellini, G.; Buonamici, S.; Cotesta, S.; Cowan-Jacob, S. W.; Dodd, S.; Drueckes, P.; Fabbro, D.; Gabriel, T.; et al. Discovery of Asciminib (ABL001), an Allosteric Inhibitor of the Tyrosine Kinase Activity of BCR-ABL1. *Journal of Medicinal Chemistry* **2018**, *61* (18), 8120-8135. DOI: 10.1021/acs.jmedchem.8b01040.
(12) Lamoree, B.; Hubbard, R. E. Using Fragment-Based Approaches to Discover New Antibiotics. *SLAS DISCOVERY: Advancing the Science of Drug Discovery* **2018**, *23* (6), 495-510. DOI: 10.1177/2472555218773034 (acccessed 2020/06/10).
(13) Brennan, P. J.; Nikaido, H. The envelope of mycobacteria. *Annu Rev Biochem* **1995**, *64*, 29-63. DOI: 10.1146/annurev.bi.64.070195.000333 From NLM.
(14) Gopal, P.; Dick, T. Reactive dirty fragments: implications for tuberculosis drug discovery. *Current Opinion in Microbiology* **2014**, *21*, 7-12. DOI: https://doi.org/10.1016/j.mib.2014.06.015.
(15) Manger, M.; Scheck, M.; Prinz, H.; von Kries, J. P.; Langer, T.; Saxena, K.; Schwalbe, H.; Fürstner, A.; Rademann, J.; Waldmann, H. Discovery of Mycobacterium Tuberculosis Protein Tyrosine Phosphatase A (MptpA) Inhibitors Based on Natural Products and a Fragment-Based Approach. *ChemBioChem* **2005**, *6* (10), 1749-1753. DOI: 10.1002/cbic.200500171 (acccessed 2020/06/11). Rawls, K. A.; Lang, P. T.; Takeuchi, J.; Imamura, S.; Baguley, T. D.; Grundner, C.; Alber, T.; Ellman, J. A. Fragment-based discovery of selective inhibitors of the Mycobacterium tuberculosis protein tyrosine phosphatase PtpA. *Bioorganic & medicinal chemistry letters* **2009**, *19* (24), 6851-6854. DOI: 10.1016/j.bmcl.2009.10.090 PubMed. Soellner, M. B.; Rawls, K. A.; Grundner, C.; Alber, T.; Ellman, J. A. Fragment-Based Substrate Activity Screening Method for the Identification of Potent Inhibitors of the Mycobacterium tuberculosis Phosphatase PtpB. *Journal of the American Chemical Society* **2007**, *129* (31), 9613-9615. DOI: 10.1021/ja0727520.

(16) Marchetti, C.; Chan, D. S. H.; Coyne, A. G.; Abell, C. Fragment-based approaches to TB drugs. *Parasitology* **2018**, *145* (2), 184-195. DOI: 10.1017/S0031182016001876 From Cambridge University Press Cambridge Core. Mendes, V.; Blundell, T. L. Targeting tuberculosis using structure-guided fragment-based drug design. *Drug Discovery Today* **2017**, *22* (3), 546-554. DOI: https://doi.org/10.1016/j.drudis.2016.10.003.
(17) Marrakchi, H.; Lanéelle, M. A.; Daffé, M. Mycolic acids: structures, biosynthesis, and beyond. *Chem Biol* **2014**, *21* (1), 67-85. DOI: 10.1016/j.chembiol.2013.11.011 From NLM.
(18) Banerjee, A.; Dubnau, E.; Quemard, A.; Balasubramanian, V.; Um, K. S.; Wilson, T.; Collins, D.; de Lisle, G.; Jacobs, W. R., Jr. inhA, a gene encoding a target for isoniazid and ethionamide in Mycobacterium tuberculosis. *Science (New York, N.Y.)* **1994**, *263* (5144), 227-230. DOI: 10.1126/science.8284673 From NLM. Vilchèze, C.; Wang, F.; Arai, M.; Hazbón, M. H.; Colangeli, R.; Kremer, L.; Weisbrod, T. R.; Alland, D.; Sacchettini, J. C.; Jacobs, W. R., Jr. Transfer of a point mutation in Mycobacterium tuberculosis inhA resolves the target of isoniazid. *Nat Med* **2006**, *12* (9), 1027-1029. DOI: 10.1038/nm1466 From NLM. Wang, F.; Langley, R.; Gulten, G.; Dover, L. G.; Besra, G. S.; Jacobs, W. R., Jr.; Sacchettini, J. C. Mechanism of thioamide drug action against tuberculosis and leprosy. *J Exp Med* **2007**, *204* (1), 73-78. DOI: 10.1084/jem.20062100 From NLM.
(19) Baulard, A. R.; Betts, J. C.; Engohang-Ndong, J.; Quan, S.; Brennan, P. J.; Locht, C.; Besra, G. S. Activation of the pro-drug ethionamide is regulated in mycobacteria. *Journal of Biological Chemistry* **2000**. DOI: 10.1074/jbc.M003744200. Grant, S. S.; Wellington, S.; Kawate, T.; Desjardins, C. A.; Silvis, M. R.; Wivagg, C.; Thompson, M.; Gordon, K.; Kazyanskaya, E.; Nietupski, R.; et al. Baeyer-Villiger Monooxygenases EthA and MymA Are Required for Activation of Replicating and Non-replicating Mycobacterium tuberculosis Inhibitors. *Cell Chem Biol* **2016**, *23* (6), 666-677. DOI: 10.1016/j.chembiol.2016.05.011. Flipo, M.; Frita, R.; Bourotte, M.; Martínez-Martínez, M. S.; Boesche, M.; Boyle, G. W.; Derimanov, G.; Drewes, G.; Gamallo, P.; Ghidelli-Disse, S.; et al. The small-molecule SMARt751 reverses Mycobacterium tuberculosis resistance to ethionamide in acute and chronic mouse models of tuberculosis. *Science Translational Medicine* **2022**, *14* (643), eaaz6280. DOI: doi:10.1126/scitranslmed.aaz6280.
(20) Frénois, F.; Engohang-Ndong, J.; Locht, C.; Baulard, A. R.; Villeret, V. Structure of EthR in a ligand bound conformation reveals therapeutic perspectives against tuberculosis. *Mol Cell* **2004**, *16* (2), 301-307. DOI: 10.1016/j.molcel.2004.09.020 From NLM.
(21) Dover, L. G.; Corsino, P. E.; Daniels, I. R.; Cocklin, S. L.; Tatituri, V.; Besra, G. S.; Fütterer, K. Crystal Structure of the TetR/CamR Family Repressor Mycobacterium tuberculosis EthR Implicated in Ethionamide Resistance. *Journal of Molecular Biology* **2004**, *340* (5), 1095-1105. DOI: https://doi.org/10.1016/j.jmb.2004.06.003.
(22) Flipo, M.; Desroses, M.; Lecat-Guillet, N.; Dirié, B.; Carette, X.; Leroux, F.; Piveteau, C.; Demirkaya, F.; Lens, Z.; Rucktooa, P.; et al. Ethionamide Boosters: Synthesis, Biological Activity, and Structure−Activity Relationships of a Series of 1,2,4-Oxadiazole EthR Inhibitors. *Journal of Medicinal Chemistry* **2011**, *54* (8), 2994-3010. DOI: 10.1021/jm200076a (acccessed 2014/12/17). Flipo, M.; Desroses, M.; Lecat-Guillet, N.; Villemagne, B.; Blondiaux, N.; Leroux, F.; Piveteau, C.; Mathys, V.; Flament, M.-P.; Siepmann, J.; et al. Ethionamide Boosters. 2. Combining Bioisosteric Replacement and Structure-Based Drug Design To Solve Pharmacokinetic Issues in a Series of Potent 1,2,4-Oxadiazole EthR Inhibitors. *Journal of Medicinal Chemistry* **2011**, *55* (1), 68-83. DOI: 10.1021/jm200825u (acccessed 2014/12/17). Flipo, M.; Willand, N.; Lecat-Guillet, N.; Hounsou, C.; Desroses, M.; Leroux, F.; Lens, Z.; Villeret, V.; Wohlkönig, A.; Wintjens, R.; et al. Discovery of Novel N-Phenylphenoxyacetamide Derivatives as EthR Inhibitors and Ethionamide Boosters by Combining High-Throughput Screening and Synthesis. *Journal of Medicinal Chemistry* **2012**, *55* (14), 6391-6402. DOI: 10.1021/jm300377g (acccessed 2014/12/17).
(23) Willand, N.; Dirie, B.; Carette, X.; Bifani, P.; Singhal, A.; Desroses, M.; Leroux, F.; Willery, E.; Mathys, V.; Deprez-Poulain, R.; et al. Synthetic EthR inhibitors boost antituberculous activity of ethionamide. *Nature Medicine* **2009**, *15* (5), 537-544, 10.1038/nm.1950. DOI: 10.1038/nm.1950.
(24) Willand, N.; Flipo, M.; Villemagne, B.; Baulard, A.; Deprez, B. Chapter Five - Recent advances in the design of inhibitors of mycobacterial transcriptional regulators to boost thioamides anti-

tubercular activity and circumvent acquired-resistance. In *Annual Reports in Medicinal Chemistry*, Chibale, K. Ed.; Vol. 52; Academic Press, 2019; pp 131-152.
(25) Surade, S.; Ty, N.; Hengrung, N.; Lechartier, B.; Cole, Stewart T.; Abell, C.; Blundell, Tom L. A structure-guided fragment-based approach for the discovery of allosteric inhibitors targeting the lipophilic binding site of transcription factor EthR. *Biochemical Journal* **2014**, *458* (2), 387. DOI: 10.1042/BJ20131127. Nikiforov, P. O.; Surade, S.; Blaszczyk, M.; Delorme, V.; Brodin, P.; Baulard, A. R.; Blundell, T. L.; Abell, C. A fragment merging approach towards the development of small molecule inhibitors of Mycobacterium tuberculosis EthR for use as ethionamide boosters. *Org Biomol Chem* **2016**, *14* (7), 2318-2326. DOI: 10.1039/c5ob02630j.
(26) Nikiforov, P. O.; Blaszczyk, M.; Surade, S.; Boshoff, H. I.; Sajid, A.; Delorme, V.; Deboosere, N.; Brodin, P.; Baulard, A. R.; Barry, C. E.; et al. Fragment-Sized EthR Inhibitors Exhibit Exceptionally Strong Ethionamide Boosting Effect in Whole-Cell Mycobacterium tuberculosis Assays. *ACS Chem Biol* **2017**, *12* (5), 1390-1396. DOI: 10.1021/acschembio.7b00091.
(27) Villemagne, B.; Flipo, M.; Blondiaux, N.; Crauste, C.; Malaquin, S.; Leroux, F.; Piveteau, C.; Villeret, V.; Brodin, P.; Villoutreix, B. O.; et al. Ligand Efficiency Driven Design of New Inhibitors of Mycobacterium tuberculosis Transcriptional Repressor EthR Using Fragment Growing, Merging, and Linking Approaches. *Journal of Medicinal Chemistry* **2014**, *57* (11), 4876-4888. DOI: 10.1021/jm500422b (acccessed 2014/12/17).
(28) Villemagne, B.; Machelart, A.; Tran, N. C.; Flipo, M.; Moune, M.; Leroux, F.; Piveteau, C.; Wohlkönig, A.; Wintjens, R.; Li, X.; et al. Fragment-Based Optimized EthR Inhibitors with in Vivo Ethionamide Boosting Activity. *ACS Infectious Diseases* **2020**, *6* (3), 366-378. DOI: 10.1021/acsinfecdis.9b00277.
(29) Blondiaux, N.; Moune, M.; Desroses, M.; Frita, R.; Flipo, M.; Mathys, V.; Soetaert, K.; Kiass, M.; Delorme, V.; Djaout, K.; et al. Reversion of antibiotic resistance in Mycobacterium tuberculosis by spiroisoxazoline SMARt-420. *Science (New York, N.Y.)* **2017**, *355* (6330), 1206-1211, 10.1126/science.aag1006. DOI: 10.1126/science.aag1006.
(30) Prevet, H.; Moune, M.; Tanina, A.; Kemmer, C.; Herledan, A.; Frita, R.; Wohlkonig, A.; Bourotte, M.; Villemagne, B.; Leroux, F.; et al. A fragment-based approach towards the discovery of N-substituted tropinones as inhibitors of Mycobacterium tuberculosis transcriptional regulator EthR2. *European journal of medicinal chemistry* **2019**, *167*, 426-438. DOI: 10.1016/j.ejmech.2019.02.023.
(31) Rožman, K.; Sosič, I.; Fernandez, R.; Young, R. J.; Mendoza, A.; Gobec, S.; Encinas, L. A new 'golden age' for the antitubercular target InhA. *Drug Discov Today* **2017**, *22* (3), 492-502. DOI: 10.1016/j.drudis.2016.09.009 From NLM.
(32) Prati, F.; Zuccotto, F.; Fletcher, D.; Convery, M. A.; Fernandez-Menendez, R.; Bates, R.; Encinas, L.; Zeng, J.; Chung, C. W.; De Dios Anton, P.; et al. Screening of a Novel Fragment Library with Functional Complexity against Mycobacterium tuberculosis InhA. *ChemMedChem* **2018**, *13* (7), 672-677. DOI: 10.1002/cmdc.201700774 From NLM.
(33) Sabbah, M.; Mendes, V.; Vistal, R. G.; Dias, D. M. G.; Záhorszká, M.; Mikušová, K.; Korduláková, J.; Coyne, A. G.; Blundell, T. L.; Abell, C. Fragment-Based Design of Mycobacterium tuberculosis InhA Inhibitors. *Journal of Medicinal Chemistry* **2020**, *63* (9), 4749-4761. DOI: 10.1021/acs.jmedchem.0c00007.
(34) Sabbah, M.; Mendes, V.; Vistal, R. G.; Dias, D. M. G.; Záhorszká, M.; Mikušová, K.; Korduláková, J.; Coyne, A. G.; Blundell, T. L.; Abell, C. Correction to Fragment-Based Design of Mycobacterium tuberculosis InhA Inhibitors. *Journal of Medicinal Chemistry* **2020**, *63* (15), 8650-8650. DOI: 10.1021/acs.jmedchem.0c01187.
(35) Marrakchi, H.; Ducasse, S.; Labesse, G.; Montrozier, H.; Margeat, E.; Emorine, L.; Charpentier, X.; Daffé, M.; Quémard, A. K. MabA (FabG1), a Mycobacterium tuberculosis protein involved in the long-chain fatty acid elongation system FAS-II. *Microbiology (Reading)* **2002**, *148* (Pt 4), 951-960. DOI: 10.1099/00221287-148-4-951.
(36) Faïon, L.; Djaout, K.; Frita, R.; Pintiala, C.; Cantrelle, F.-X.; Moune, M.; Vandeputte, A.; Bourbiaux, K.; Piveteau, C.; Herledan, A.; et al. Discovery of the first Mycobacterium tuberculosis MabA (FabG1)

inhibitors through a fragment-based screening. *European Journal of Medicinal Chemistry* **2020**, *200*, 112440. DOI: https://doi.org/10.1016/j.ejmech.2020.112440.
(37) Prevet, H.; Flipo, M.; Roussel, P.; Deprez, B.; Willand, N. Microwave-assisted synthesis of functionalized spirohydantoins as 3-D privileged fragments for scouting the chemical space. *Tetrahedron Letters* **2016**, *57* (26), 2888-2894. DOI: https://doi.org/10.1016/j.tetlet.2016.05.065.
Tran, N. C.; Dhondt, H.; Flipo, M.; Deprez, B.; Willand, N. Synthesis of functionalized 2-isoxazolines as three-dimensional fragments for fragment-based drug discovery. *Tetrahedron Letters* **2015**, *56* (27), 4119-4123. DOI: https://doi.org/10.1016/j.tetlet.2015.05.035.
(38) Cole, S. T.; Brosch, R.; Parkhill, J.; Garnier, T.; Churcher, C.; Harris, D.; Gordon, S. V.; Eiglmeier, K.; Gas, S.; Barry, C. E.; et al. Deciphering the biology of Mycobacterium tuberculosis from the complete genome sequence. *Nature* **1998**, *393* (6685), 537-544. DOI: 10.1038/31159.
(39) Beste, D. J. V.; Espasa, M.; Bonde, B.; Kierzek, A. M.; Stewart, G. R.; McFadden, J. The Genetic Requirements for Fast and Slow Growth in Mycobacteria. *PLOS ONE* **2009**, *4* (4), e5349. DOI: 10.1371/journal.pone.0005349.
(40) Banerjee, D. R.; Dutta, D.; Saha, B.; Bhattacharyya, S.; Senapati, K.; Das, A. K.; Basak, A. Design, synthesis and characterization of novel inhibitors against mycobacterial β-ketoacyl CoA reductase FabG4. *Organic & Biomolecular Chemistry* **2014**, *12* (1), 73-85, 10.1039/C3OB41676C. DOI: 10.1039/C3OB41676C.
(41) Tasdemir, D.; Lack, G.; Brun, R.; Rüedi, P.; Scapozza, L.; Perozzo, R. Inhibition of Plasmodium falciparum Fatty Acid Biosynthesis: Evaluation of FabG, FabZ, and FabI as Drug Targets for Flavonoids. *Journal of Medicinal Chemistry* **2006**, *49* (11), 3345-3353. DOI: 10.1021/jm0600545.
Zhang, Y.-M.; Rock, C. O. Evaluation of Epigallocatechin Gallate and Related Plant Polyphenols as Inhibitors of the FabG and FabI Reductases of Bacterial Type II Fatty-acid Synthase *. *Journal of Biological Chemistry* **2004**, *279* (30), 30994-31001. DOI: 10.1074/jbc.M403697200 (acccessed 2021/05/20).
(42) Chen, L.; Wilson, D. J.; Xu, Y.; Aldrich, C. C.; Felczak, K.; Sham, Y. Y.; Pankiewicz, K. W. Triazole-Linked Inhibitors of Inosine Monophosphate Dehydrogenase from Human and Mycobacterium tuberculosis. *Journal of Medicinal Chemistry* **2010**, *53* (12), 4768-4778. DOI: 10.1021/jm100424m.
(43) Huennekens, F. M. Folic Acid Coenzymes in the Biosynthesis of Purines and Pyrimidines. In *Vitamins & Hormones*, Harris, R. S., Wool, I. G., Loraine, J. A., Thimann, K. V. Eds.; Vol. 26; Academic Press, 1969; pp 375-394.
(44) Shelke, R. U.; Degani, M. S.; Raju, A.; Ray, M. K.; Rajan, M. G. Fragment Discovery for the Design of Nitrogen Heterocycles as Mycobacterium tuberculosis Dihydrofolate Reductase Inhibitors. *Arch Pharm (Weinheim)* **2016**, *349* (8), 602-613. DOI: 10.1002/ardp.201600066 From NLM.
(45) Ribeiro, J. A.; Hammer, A.; Libreros-Zúñiga, G. A.; Chavez-Pacheco, S. M.; Tyrakis, P.; de Oliveira, G. S.; Kirkman, T.; El Bakali, J.; Rocco, S. A.; Sforça, M. L.; et al. Using a Fragment-Based Approach to Identify Alternative Chemical Scaffolds Targeting Dihydrofolate Reductase from Mycobacterium tuberculosis. *ACS Infectious Diseases* **2020**, *6* (8), 2192-2201. DOI: 10.1021/acsinfecdis.0c00263.
(46) Trapero, A.; Pacitto, A.; Singh, V.; Sabbah, M.; Coyne, A. G.; Mizrahi, V.; Blundell, T. L.; Ascher, D. B.; Abell, C. Fragment-Based Approach to Targeting Inosine-5'-monophosphate Dehydrogenase (IMPDH) from Mycobacterium tuberculosis. *Journal of Medicinal Chemistry* **2018**, *61* (7), 2806-2822. DOI: 10.1021/acs.jmedchem.7b01622.
(47) Usha, V.; Hobrath, J. V.; Gurcha, S. S.; Reynolds, R. C.; Besra, G. S. Identification of Novel Mt-Guab2 Inhibitor Series Active against M. tuberculosis. *PLOS ONE* **2012**, *7* (3), e33886. DOI: 10.1371/journal.pone.0033886.
(48) Huang, H. L.; Krieger, I. V.; Parai, M. K.; Gawandi, V. B.; Sacchettini, J. C. Mycobacterium tuberculosis Malate Synthase Structures with Fragments Reveal a Portal for Substrate/Product Exchange. *J Biol Chem* **2016**, *291* (53), 27421-27432. DOI: 10.1074/jbc.M116.750877 From NLM.
(49) Krieger, I. V.; Freundlich, J. S.; Gawandi, V. B.; Roberts, J. P.; Sun, Q.; Owen, J. L.; Fraile, M. T.; Huss, S. I.; Lavandera, J. L.; Ioerger, T. R.; et al. Structure-guided discovery of phenyl-diketo acids as potent inhibitors of M. tuberculosis malate synthase. *Chem Biol* **2012**, *19* (12), 1556-1567. DOI: 10.1016/j.chembiol.2012.09.018 From NLM.

(50) Abreu, R.; Giri, P.; Quinn, F. Host-Pathogen Interaction as a Novel Target for Host-Directed Therapies in Tuberculosis. *Frontiers in Immunology* **2020**, *11* (1553), Review. DOI: 10.3389/fimmu.2020.01553.
(51) Ouellet, H.; Johnston, J. B.; Montellano, P. R. O. d. Cholesterol catabolism as a therapeutic target in Mycobacterium tuberculosis. *Trends in Microbiology* **2011**, *19* (11), 530-539. DOI: 10.1016/j.tim.2011.07.009 (acccessed 2021/09/07).
(52) Pandey, A. K.; Sassetti, C. M. Mycobacterial persistence requires the utilization of host cholesterol. *Proceedings of the National Academy of Sciences* **2008**, *105* (11), 4376-4380. DOI: 10.1073/pnas.0711159105.
(53) Rengarajan, J.; Bloom, B. R.; Rubin, E. J. Genome-wide requirements for Mycobacterium tuberculosis adaptation and survival in macrophages. *Proceedings of the National Academy of Sciences of the United States of America* **2005**, *102* (23), 8327-8332. DOI: 10.1073/pnas.0503272102.
(54) Ryan, A.; Polycarpou, E.; Lack, N. A.; Evangelopoulos, D.; Sieg, C.; Halman, A.; Bhakta, S.; Eleftheriadou, O.; McHugh, T. D.; Keany, S.; et al. Investigation of the mycobacterial enzyme HsaD as a potential novel target for anti-tubercular agents using a fragment-based drug design approach. *Br J Pharmacol* **2017**, *174* (14), 2209-2224. DOI: 10.1111/bph.13810 From NLM.
(55) Ryan, A.; Keany, S.; Eleftheriadou, O.; Ballet, R.; Cheng, H. Y.; Sim, E. Mechanism-based inhibition of HsaD: a C-C bond hydrolase essential for survival of Mycobacterium tuberculosis in macrophage. *FEMS Microbiol Lett* **2014**, *350* (1), 42-47. DOI: 10.1111/1574-6968.12302 From NLM.
(56) Payne, D. J.; Gwynn, M. N.; Holmes, D. J.; Pompliano, D. L. Drugs for bad bugs: confronting the challenges of antibacterial discovery. *Nature Reviews Drug Discovery* **2007**, *6* (1), 29-40. DOI: 10.1038/nrd2201.
(57) Koul, A.; Arnoult, E.; Lounis, N.; Guillemont, J.; Andries, K. The challenge of new drug discovery for tuberculosis. *Nature* **2011**, *469* (7331), 483-490. DOI: 10.1038/nature09657 From NLM.
(58) Barry, C. E.; Boshoff, H. I.; Dartois, V.; Dick, T.; Ehrt, S.; Flynn, J.; Schnappinger, D.; Wilkinson, R. J.; Young, D. The spectrum of latent tuberculosis: rethinking the biology and intervention strategies. *Nature Reviews Microbiology* **2009**, *7* (12), 845-855. DOI: 10.1038/nrmicro2236.
(59) Moreira, W.; Lim, J. J.; Yeo, S. Y.; Ramanujulu, P. M.; Dymock, B. W.; Dick, T. Fragment-Based Whole Cell Screen Delivers Hits against M. tuberculosis and Non-tuberculous Mycobacteria. *Frontiers in Microbiology* **2016**, *7*, 1392, 10.3389/fmicb.2016.01392.